Time-Domain Shielding Effectiveness of Enclosures against a Plane Wave Excitation

Luis Ginés García-Pérez, Antonio José Lozano-Guerrero, *Member, IEEE*, Juan M. Blázquez-Ruíz, Juan F. Valenzuela-Valdés, Juan Monzó-Cabrera, José Fayos-Fernández and Alejandro Díaz-Morcillo, *Senior Member, IEEE*

***Abstract*— Electromagnetic shielding of metallic enclosures with an aperture are simulated and measured in the frequency and time domain in this paper. Recently, several new figures of shielding effectiveness (SE) in the time domain have been proposed. Much work has been done regarding numerical simulations however little related to measurements has been carried out. In this work, we obtain the simulated and measured results for these SE definitions when an incident plane wave, with a determined bandwidth, excites the enclosure. The plane wave can be treated as a reference interference to compare with other cases. Measurements and simulations are in good agreement. This study evaluates the new definitions and compares them with the classical definition in the frequency domain. The effect of the probes, a dipole or a loop, has also been analyzed. Finally, the SE values are obtained for a sweep of the size of the aperture providing a unique value of equivalent SE for the most critical parameter and for a determined bandwidth, and allowing direct comparison with other enclosures.**

***Index Terms*—Apertures, electrical equipment enclosures, numerical analysis, shielding, time-domain analysis.**

I. Introduction

Traditionally, multiple definitions to describe and evaluate the electromagnetic shielding have been used [1-4], as well as rules and standards [5-6]. The study of the shielding provided by metallic enclosures with apertures and drillings for input and output devices is very wide [7-10]. In order to approach this study, analytical or semi-analytical techniques have been applied [11-13]. Numerical methods can deal with any kind of enclosure and inner contents [14-17]. In the Time-Domain (TD) we find the Transmission-Line Modelling Method (TLM) [18], Finite-Difference Time-Domain Method (FDTD) [19-21] and Finite-Integration Technique (FIT) [22] among others. Finite Element Method (FEM) [23] is the most popular Frequency-Domain (FD) numerical method.

The electromagnetic shielding of enclosures against radiated interferences and the TD and FD studies require determining specific parameters for measuring the shielding effectiveness. With this purpose, there are recent essays that use indicators based on the TD response to study the peak reduction of the electric field intensity, magnetic field intensity and energy density [23-25].

The objectives in this work are:

1) to simulate recent and classical SE indicators of an enclosure with an aperture with a normally impinging plane wave,
2) to reproduce the set-ups in the laboratory to obtain the equivalent measurements,
3) to compare measurements and simulations to verify the reproducibility of the recently proposed SE equivalent parameter for a plane wave in a determined bandwidth,
4) and to simulate the system when the aperture is sequentially modified for both width and length, in order to obtain results and conclusions.

In addition, a goal of this paper is to assess if a TD study of this characteristics is meaningful to study the SE produced by an incident plane wave on an enclosure.

Although almost all potential interference sources are at narrow band frequencies there are sources with broadband spectra such as digital waveforms or even if there is going to be inner electrical equipment, working at several frequencies, this kind of analysis may be meaningful and help to choose easily in between two or more enclosure configurations. Concerning the levels, although commercial limits for radiated field immunity are really low, only 3V/m, and for Network Equipment Building Standards (NEBS) is 10V/m (IEC/EN-61000-4-3) there are high intensity interferences such as electromagnetic pulses (EMP) or lightning [1] that can reach very high levels of electric field and this can be helpful for military applications

II. Theory

Generally, most of electric and electronic devices are sensitive to one or more of the following physical quantities [24-26]: the maximum value of the electric and/or magnetic field, the maximum value of induced effects caused by the time variations of magnetic and/or electric flux density, and the total

Manuscript received August 4, 2016; revised October 5, 2016; Accepted October 28, 2016.

Luis Ginés García-Pérez, Antonio José Lozano-Guerrero, Juan M. Blázquez-Ruíz, Juan Monzó-Cabrera, José Fayos Fernández and Alejandro Díaz-Morcillo are with the Departamento de Tecnologías de la Información y las Comunicaciones of Universidad Politécnica de Cartagena, Cartagena, E-30202, Spain (phone; +34968326468 fax: +34968325973 e-mail: antonio.lozano@upct.es).

Juan F. Valenzuela-Valdés is with the Department of Signal, Theory Telematics and Communications, Universidad de Granada, Granada, Spain.

energy delivered. The SE in the observation point will depend on polarizations and angles of incidence for every specific system. However, in this study only the usual empty most critical scenario is studied [11].

In 2013 a new IEEE Standard Method [5] was approved, and like in the IEEE Standard 299-1997 [6] the classical definitions of SE are included. For low frequencies in [6] (50Hz to 20MHz) it is included among others parameters, the magnetic field magnitude $|H_s|$ inside an enclosure with the field $|H_{in}|$ at the same observation point in absence of such an enclosure as:

$$SE_H = 20\, log_{10} \frac{|H_{in}|}{|H_S|} \text{ (dB)} \quad (1)$$

For resonant range frequencies (from 20 to 300 MHz), this classic standard [6] defined the electric field SE as the relationship between the electric field magnitude $|E_s|$ inside the enclosure and the field $|E_{in}|$ at the same observation point without enclosure:

$$SE_E = 20\, log_{10} \frac{|E_{in}|}{|E_S|} \text{ (dB)} \quad (2)$$

In the high-frequency case, i.e., when the dimensions of the shield are comparable or larger to the wave-length, the attenuation of the electromagnetic field (rather than of the electric and magnetic fields alone) has to be considered [27]. Therefore, for higher frequencies (upper than 1.7GHz) the relation between the received power into the enclosure P_s and without enclosure P_{in} was defined as follows:

$$SE_P = 10\, log_{10} \frac{P_{in}}{P_S} \text{ (dB)} \quad (3)$$

In the definitions above the numerator is the peak value of the incident field "*in*" in the observation point in absence of the enclosure, while the denominator defines the peak value of the field in the shielded zone "*s*" in the same observation point.

The following definitions have been recently proposed in the time-domain.

A. Peak Reduction Shielding Effectiveness

This parameter is useful to account for the transient behavior of shields, however we will obtain its value from the TD plane wave excitation to obtain an equivalent SE in the bandwidth under study. It is based on the peak reduction in the waveform and accounts for the performance of structures designed to protect systems sensitive to an EM field higher than a fixed threshold. It may be referenced to the electric and magnetic field, as it follows:

$$SE_{E\_PR} = 20 \log \frac{\left|E^{in}_{MAX}(t,x,y,z)\right|}{\left|E^{s}_{MAX}(t,x,y,z)\right|} \quad (4)$$

$$SE_{H\_PR} = 20 \log \frac{\left|H^{in}_{MAX}(t,x,y,z)\right|}{\left|H^{s}_{MAX}(t,x,y,z)\right|} \quad (5)$$

It should be noted that the peak value is for the absolute value of the field [28].

B. Derivative Reduction Shielding Effectiveness

It is the reduction of the EM field time derivate in the shielded region. It evaluates the limitation of the induced effects due to, according to Maxwell equations, time derivative of magnetic or electric flux density, denoted as $\dot{B}(t,x,y,z), \dot{D}(t,x,y,z)$, respectively [28]:

$$SE_{B\_DR} = 20 \log \frac{\left|\dot{B}^{in}_{MAX}(t,x,y,z)\right|}{\left|\dot{B}^{s}_{MAX}(t,x,y,z)\right|} \quad (6)$$

$$SE_{D\_DR} = 20 \log \frac{\left|\dot{D}^{in}_{MAX}(t,x,y,z)\right|}{\left|\dot{D}^{s}_{MAX}(t,x,y,z)\right|} \quad (7)$$

In (6) the magnetic flux density or magnetic induction relates with the magnetic field intensity through the magnetic permeability:

$$\vec{B}(t,x,y,z) = \mu(x,y,z)\, \vec{H}(t,x,y,z) \quad (8)$$

In (7) the electric flux density relates with the electric field intensity through the electric permittivity:

$$\vec{D}(t,x,y,z) = \varepsilon(x,y,z)\, \vec{E}(t,x,y,z) \quad (9)$$

C. Energy Reduction Shielding Effectiveness

This is the reduction of the volumetric energy density in the shielded zone. It shows the reduction of the energy that may be delivered to a device located at a given position. It requires the introduction of the energy density [25], expressed in (J/m^2):

$$W = \int_0^{\infty} \left[\left|\vec{E}(t,x,y,z) \times \vec{H}(t,x,y,z)\right|\right] dt \quad (10)$$

The upper limit in the time integral is finite in actual transients of practical interest: the improper integral will reduce to a simple integral over a finite time interval; however, the lasting of the transient may be different in presence and absence of the shielding configuration and in this paper a specific attention will be paid to its duration. The energy reduction shielding effectiveness refers to the absolute value of the energy in every case [28] and it is defined as:

$$SE_{WR} = 10 \log \frac{\left|W^{in}(x,y,z)\right|}{\left|W^{s}(x,y,z)\right|} \quad (11)$$

III. Implementation: Simulations and Measurements

Fig. 1 shows the set-up configuration to evaluate the effects of the excitation of an incident plane wave with the proposed SE parameters.

The commercial code CST Microwave Studio (based on the Finite Integration Technique) using the TD solver to obtain the SE of a conductive enclosure with a rectangular aperture, as Fig. 1 shows. The considered model consists of a metallic conducting (conductivity = 10^7 S/m) shielding box illuminated by a plane wave that travels on the z axe direction and in negative sense, directly to the aperture in order to simulate the worst case [8, 11]. The enclosure dimensions are $a \times b \times c = 30\ cm \times 12\ cm \times 30\ cm$ with a $(l \times w)$ rectangular aperture

centred on the front panel (as shown in Fig. 1). The IEEE Standard 299.1-2013 [5] classifies these dimensions as "physically small". The thickness of the walls is 0.05 cm. The boundary conditions are defined as "o*pen (add space)*" in all directions, that adds some extra space to satisfy the free space radiation condition.

The mesh is defined as hexahedral type PBA ("*Perfect Boundary Approximation*"), so small details of the structure will be modelled accurately only if the mesh cell sizes are smaller than these details. The number of steps per wavelength value (λ) is 20, higher than usual values, from 4 to 10.

As there are no real losses in the enclosure, the convergence at internal resonances of the box has been guaranteed through two simulation parameters high values that control the calculation accuracy (*steadystatelimit* = -80 dB), and the time limit (*numberofpulsewidths* = 1000, even 10.000 for narrower apertures).

Discretization of the system configuration required only 58.880 cells to get good results. In fact, to verify the simulated results accuracy by CST Microwave Studio, they have been compared with different measurements in laboratory. The observation point is always located in the middle of the enclosure (coordinates (x, y, z) = (0,0,0)).

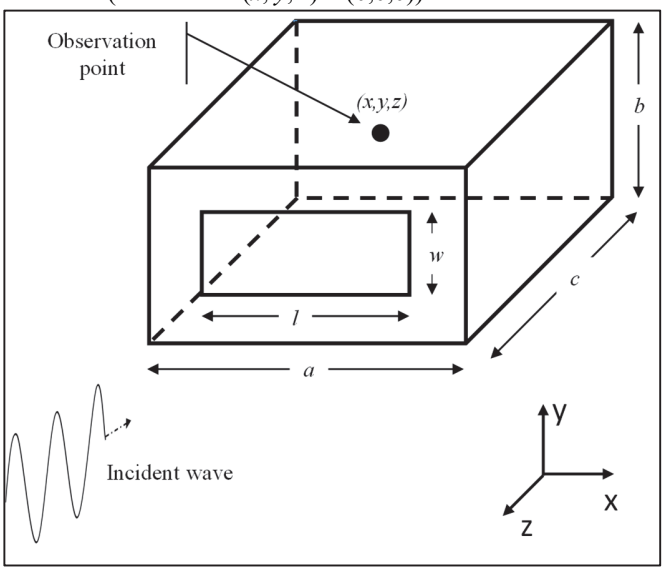

Fig. 1. System Configuration: Incident PW to an enclosure with a rectangular aperture.

Fig. 2 shows the enclosure located inside an anechoic room that has dimensions $220\ cm \times 310\ cm \times 465\ cm$ at 3 m distance, like in [11, 29], of a log-periodic antenna oriented in vertical position. In this way, the antenna emits a signal that, due to the distance to the observation point, acts like a plane wave in the frequency interval of 500 MHz to 2 GHz. The IEEE Standard 299.1-2013 [5] classifies this problem for the frequency interval under study as "electrically large" since the enclosure physical dimensions are comparable or larger than the wavelength.

The vector network analyser (VNA) Rohde & Schwarzt ZVA67 [30] was used for all the measurements. A base-power-level equal to 40dBm in order to reduce the floor noise level at low frequencies and match better the results at higher frequencies was selected.

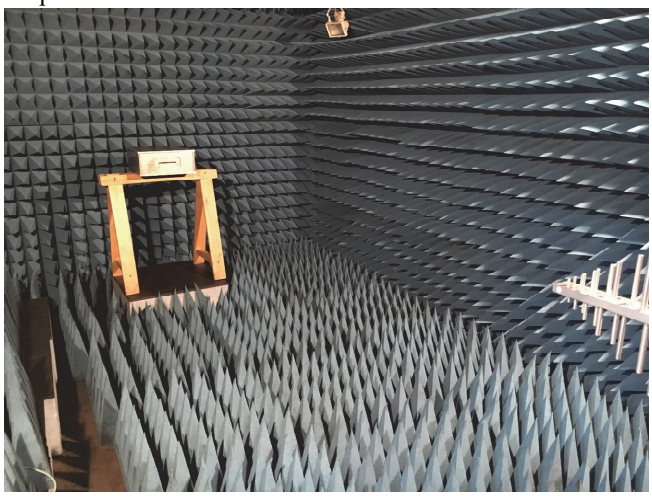

Fig. 2. Shielding enclosure with an aperture in the anechoic chamber.

Results for the measurement set up were obtained using the TD option of the VNA ZVA67 using a Hanning window. In the frequency domain 10001 points in the range 500MHz to 2 GHz, then we selected the option TD, and from the time curve, the absolute magnitude of S_{21} was selected. This could have been done from the frequency-measured data with the correspondent transformations [31].

The electric parameters were measured using an electric probe (4 *cm* long monopole) oriented in vertical position, located at the enclosure floor and centered. In the simulations, the influence of the monopole was studied.

To obtain the magnetic measurements a shielded loop as the one used in [11], with 4.5 *cm* inner diameter. The loop is located in the middle of the enclosure centered in the YZ plane.

It should be noted that in this paper the plane wave is used as a specific reference case to evaluate the time-domain SE that can be compared to other cases such as Electrostatic Discharges (ESD), Electromagnetic Pulses etc. CST Microwave Studio has generated the specific excitation plane wave for the frequency intervals from 500MHz to 2GHz.

IV. Results

A. Electric Field SE Results

Fig. 3 and 4 show a frequency domain comparison of electric field shielding effectiveness for measured and simulated results in the frequency domain. In order to do such comparison it has to be taken into account that VNA –in this case, the Rohde & Schwartz ZVA67 provides the scattering parameters [30].

Fig. 3 shows a comparison between the laboratory measurements and the simulation results provided by CST with an $10\ cm \times 0.5\ cm$ aperture, while Fig. 4 shows the analogous comparison with a total aperture ($30\ cm \times 12\ cm$).

In Fig. 3, the resonance value for the empty enclosure is 707 MHz. It does perfectly match with monopole in simulations but not in absence of it. In fact, a tighter result from 500MHz to 1300MHz is shown when the monopole is simulated inside the

enclosure. For higher frequencies, none of both adjusts properly as multimode region shows many resonances, and other reasons as the own resonance of the monopole at 1.87GHz, and its location just in the middle of the mode TE_{101} too. In order to better quantify the comparison between the measured and computed datasets the Feature Selective Validation (FSV) technique [32-34] is considered. In fact Amplitude Difference Measure (ADM) and the Feature Difference Measure (FDM) are "fair level" (0.46 and 0.69, respectively) for comparison measurements and simulation without monopole, and "fair level" too for comparison measurements and simulation with monopole. Simulations without monopole have been selected from now on. On the one hand, the presence of the monopole in the measurements is necessary, but simulations without the monopole are the ideal case. An example of how the availability of huge computational resources allows to fit resonances in presence of a monopole was studied in [21]. On the other hand, simulations without monopole are nearly 4 times faster than with monopole (in fact 4 hours against 15 hours). This is obvious since these are the smaller features and it will be needed at least a cell per the thickness of the wire, therefore it will be forced a finer mesh, which will lead to a higher computation time.

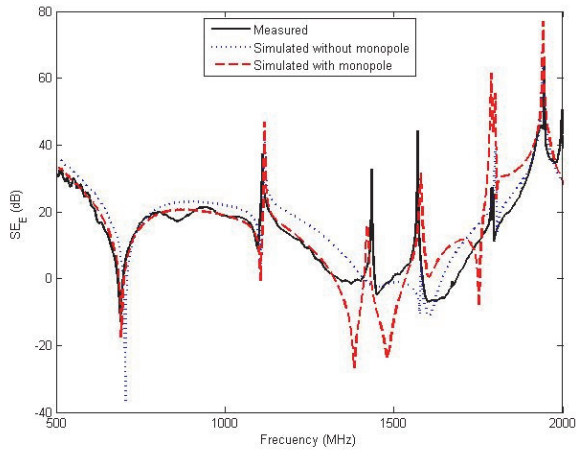

Fig. 3. Electric shielding effectiveness in the frequency domain obtained with FIT simulated without and with monopole and the results from laboratory measurements with 10 $cm \times 0.5$ cm aperture.

This variance over the y axes is not relevant in the first modes as the wave travels on the z axe. The first mode TE_{101} appears in the middle of the enclosure as a y-axe oriented cylinder at 700MHz. The second mode TE_{102} will has the same polarization and appears as two cylinders located in front and behind the middle of the enclosure at 1100MHz.

Fig. 4 reports results for the largest aperture. In this case, the problem is simpler as the front wall is eliminated [20] and the results match better than in Figure 3. As seen associated to the resonances, there are minima that produce negative levels of SE. In fact, when aperture is total, or $30\,cm \times 12\,cm$, resonances associated to the dimensions of the enclosure may lead to higher electric or magnetic field values than having no shield, and generating negative values for SE. This is because of the box resonance, and the fact that the enclosure is empty and the unique losses are due to wall conductivity and the presence of the aperture. Consequently, $30\,cm \times 12\,cm$ aperture enclosure shields worse than no enclosure. This can difficult a direct comparison between apertures in the frequency domain. Hence, at 700 MHz the shielding effectiveness of a total aperture ($30\,cm \times 12\,cm$) is slightly better than the narrower one. In fact, the ADM and the FDM are "good" and "fair" levels (0.36 and 0.50, respectively) for comparison measurements and simulation without monopole.

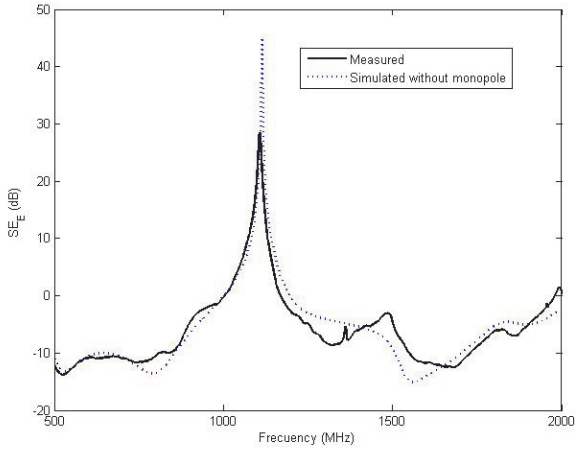

Fig. 4. Electric shielding effectiveness obtained with FIT simulated without monopole and the results from laboratory measurements with $30\,cm \times 12\,cm$.

In the time-domain [20], the shielding effectiveness can be evaluated if the electric field peak reduction is compared with and without the enclosure. With enclosure the aperture dimensions are $10\,cm \times 0.5\,cm$.

In Fig. 5, the module of the transmission parameter $|S_{21}|$ at the observation point is compared in the time domain when rectangular aperture dimensions are $10\,cm \times 0.5\,cm$ and when there is no enclosure. For this figure, the frequency range goes from 500MHz to 2GHz. Clearly, the maximum value of $|S_{21}|$ without enclosure is higher than the maximum value with enclosure. From Fig. 5 we can obtain the SE_{E_PR} in the following way:

$$SE_{E\_PR} = 20\log\frac{\left|S^{in}_{21\_MAX}(t,x,y,z)\right|}{\left|S^{s}_{21\_MAX}(t,x,y,z)\right|} \qquad (12)$$

In Fig. 6, the initial frequency of the VNA has been fixed to 500MHz and the final frequency varies from this value to 2GHz. The value of SE_{E_PR} has been obtained using (12) for the experimental result. It was necessary to change to TD before getting the maximum value of SE_{E_PR} along the time. After selecting the peak reduction maximum value in TD the results were showed for each bandwidth. Using the simulation tool, the bandwidth of the simulation varies in the same manner. As can be seen, simulations with monopole match much better than without monopole with the measurements, as the presence of the monopole affects not only because of its dimensions (its resonance at 1.87GHz), but its location just in the middle of the mode TE_{101} too, whose resonance value for the empty enclosure is 707 MHz. This effect can be appreciated from 500MHz,

which is the waveguide cut-off frequency for the TE_{10} mode.In Fig. 7, the process to get SE_{E_PR} in laboratory is the same that in Fig. 6, but the $30\ cm \times 12\ cm$ aperture speeds the simulation time and improve the SE_{E_PR} value matches between measurements and simulations. It has to be into account that simulations have been calculated without monopole. The reason for a better matching was already explained in Fig. 4.

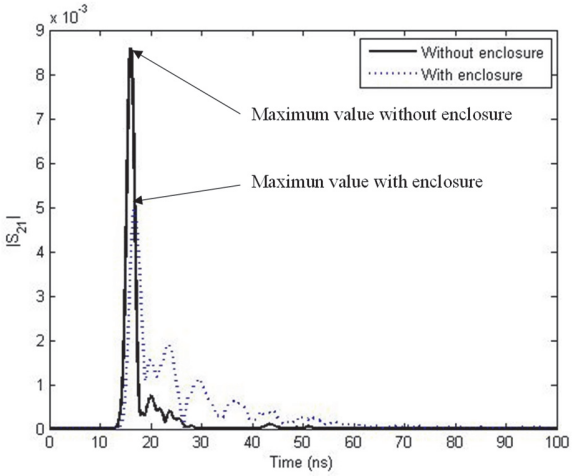

Fig. 5. Comparison of the measured $|S_{21}|$ at the observation point in TD with a $10\ cm \times 0.5\ cm$ rectangular aperture and with no enclosure.

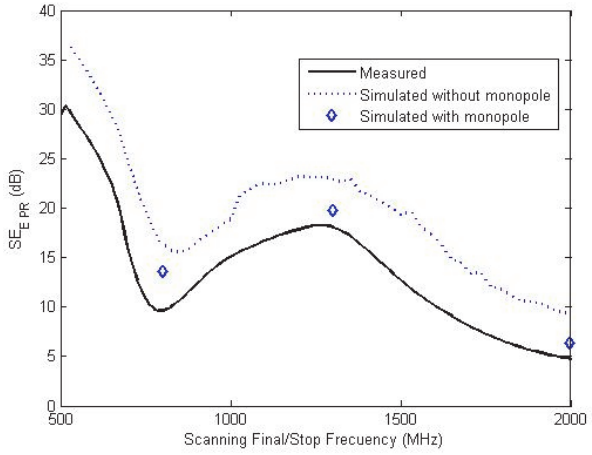

Fig. 6. Comparison of SE_{E_PR} at the observation point in TD with a $10\ cm \times 0.5\ cm$ rectangular aperture with initial scanning frequency at 500MHz.

B. *Magnetic Field SE Results*

Fig. 8 shows a comparison of magnetic field intensity shielding effectiveness for measured and simulated results without and with loop with an $10\ cm \times 0.5\ cm$ aperture.

Poor agreement is found for ADM and FDM for comparison measurements and simulation without loop, and only a slightly improvement to fair level in FDM when comparison measurements and simulation with loop are developed. Therefore, apart from the evident noise distortion at lower frequencies also present in the electric field figures, there is no significant improvement when loop is simulated. Nevertheless, simulations without loop are nearly 4 times faster than with loop, similar to the monopole case.

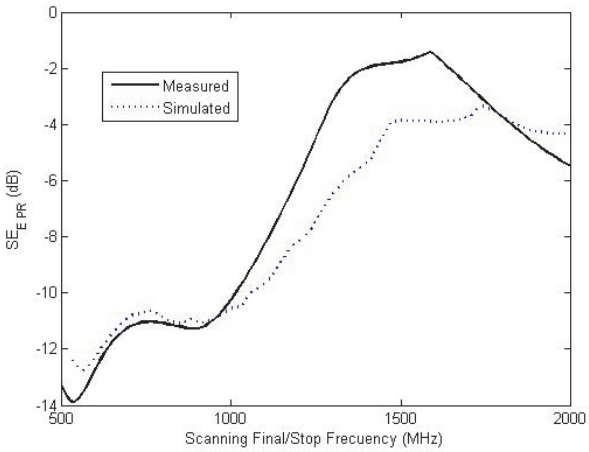

Fig. 7. Comparison of SE_{E_PR} in TD with a $(30\ cm \times 12\ cm)$ aperture.

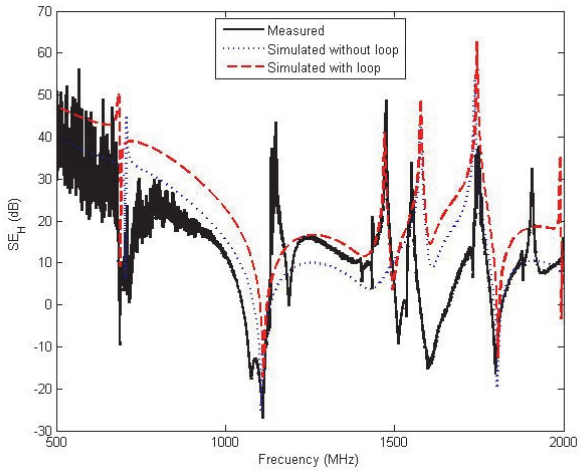

Fig. 8. Magnetic shielding effectiveness in the frequency domain obtained with FIT simulated without and with loop and the results from laboratory measurements with $10\ cm \times 0.5\ cm$ aperture.

In the time-domain, the shielding effectiveness can be evaluated if the magnetic field peak reduction is compared with and without the enclosure. We can obtain the SE_{H_PR} in the following way as previously. In Fig. 9, the initial frequency of the VNA has been fixed to 500MHz and the final frequency varies from this value to 2GHz. The value of SE_{H_PR} has been obtained for the experimental result. Using the simulation tool, the bandwidth of the simulation varies in the same manner. The result differences for figures 8 and 9 are higher due to the complexity of the loop, and may be more difficult to measure the magnetic shielding since the probe affects the field distribution. On the one hand, they allow evaluating the presence of the loop in simulations, not only as magnetic port but as an object inside the enclosure too.

On the other hand, as figure 8 and 9 compare the traditional indicators to the new suggested for different cases, and verify the new indicator as better than traditional. It is considered much more important that the grade of agreement that depends of the resonance frequencies and the presence of the loop, as new indicator corrects the irregularity of the results and it is much more reliable.

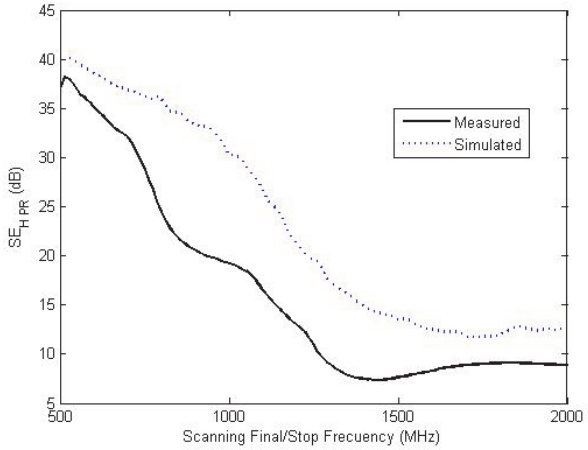

Fig. 9. Comparison of SE_{H_PR} at the observation point in TD with a 10 cm × 0.5 cm rectangular aperture.

Fig. 10 shows simulations for a 50 point bandwidth swept in which the initial frequency has been fixed to 500MHz and the final frequency varies from this value to 2GHz, and for an 10 cm × 0.5 cm aperture. The five indicators shown were defined in (4), (5), (6), (7) and (11), i.e., the TD SE for electric/magnetic field peak reduction (SE_{E_PR}, SE_{H_PR}), for electric/magnetic flux density derivative reduction (SE_{D_DR}, SE_{B_DR}), and the energy reduction SE (SE_{WR}).

The behavior of this graphic is accumulative in the sense that values at 700MHz are the results for the bandwidth from 500MHz to 700MHz, and consequently the values at 2GHz are the results for the bandwidth from 500MHz to 2GHz. Fig. 10 shows the minimum SE in time-domain for each bandwidth. As it can be seen in Figure 10 results for SE_{E_PR} and SE_{D_PR} are practically the same and this fact is reproduced for SE_{H_PR} and SE_{B_PR}. This is due to the plane wave excitation.

C. *Sequentially Modified Apertures for an Enclosure*

The selected parameter energy density (SE_{WR} [dB]) SE when varying sequentially the dimensions of the aperture is obtained.

Fig. 11 show the CST simulated results for a bandwidth from 500MHz to 2GHz, and heights and widths ranging from zero to the maximum value of the enclosure with steps of 2 and 3 cm, respectively.

Fig. 11 indicates for what apertures the final energy density SE is obtained (SE_{WR} [dB] > 0), and what apertures it is not (SE_{WR} [dB] < 0). These values have been obtained for the center of the cavity but similar studies may be carried out for the Global Shielding Effectiveness definition [35].

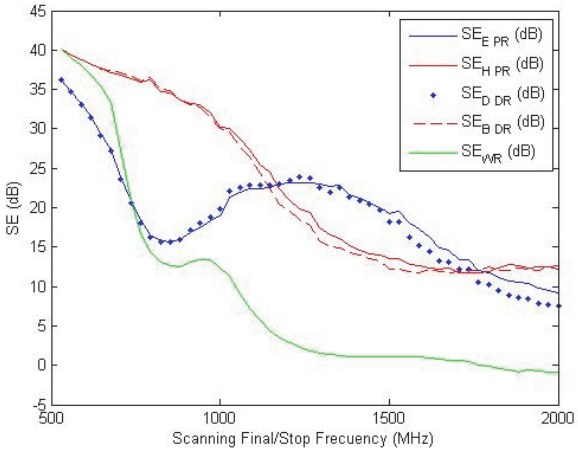

Fig. 10. Comparison of SE_{E_PR}, SE_{H_PR}, SE_{D_PR}, SE_{B_PR} and SE_{WR} simulations at the observation point in TD with a a 10 cm × 0.5 cm rectangular aperture.

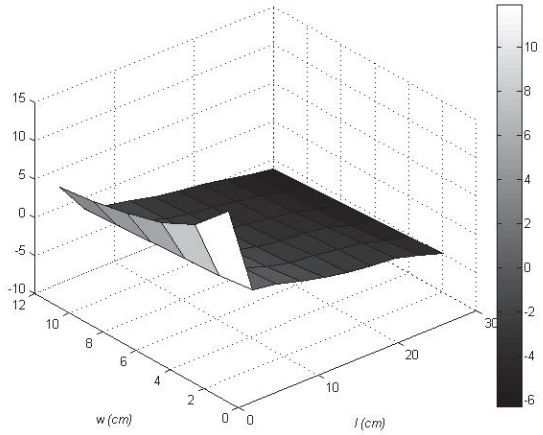

Fig. 11. SE_{WR} [dB] simulation in function of the aperture dimensions.

V. Conclusions

The recently proposed shielding effectiveness parameters in the time domain (SE_{E_PR}, SE_{H_PR}, SE_{D_DR}, SE_{B_DR}, SE_{WR}) have been obtained for a plane wave excitation in a bandwidth swept. The accumulative character of the results has to be taken into account, as results are softer than those results obtained only for a specific bandwidth in FD:

- A unique SE value represents the behavior of a specific enclosure and direct comparisons can be made with other shields to select the best in a determined bandwidth.
- The influence of the resonances is diminished.

Using each one of these TD indicators for a fixed bandwidth, it is possible to compare different systems (enclosures, sizes, apertures, observation points, …).

A comparison between the five TD indicators shows that:

- As discrepancies for electric field are lower than for

magnetic field, the reliability of the electric field indicators are better

- From SE_{E_PR}, SE_{H_PR}, and SE_{WR} indicators, the SE_{WR} indicator is the most resctrictive. Because of this, the SE_{WR} indicator is recommended against the others.
- For the practical cases, it is interesting to use the SE_{WR} parameter, as it combines both field distributions.
- The proposed TD SE_{WR} parameter can be used alternatively to the proposed FD SE parameter from IEEE Standard 299.1-2013 for physically small and electrically large enclosures, which is based on the power levels.

The proposed indicator is less time-consuming when using simulation tools than the others such as ESD of EMP due to the simplicity of the set up and can be easily measured. It does not replace them, but it supplies additional information.

The next step is to include representative contents in the enclosure, and more work is envisaged in this direction.

REFERENCES

[1] C. R. Paul, "Introduction to electromagnetic compatibility", Department of Electrical Engineering, University of Kentucky, Lexinton, 2º Edition John Wiley & Sons, 1992 New York.

[2] S. Celozzi, R. Araneo and G. Lovat, "Electromagnetic Shielding", Electrical Engineering Department "La Sapienza" University, Rome, Italy. 2008 John Wiley & Sons, Inc.

[3] S. M. Ward, J. F. Dawson and A. C. Marvn, "Towards an improved definition of electromagnetic shielding effectiveness", Proc. EMC 2000 Brugge, September 2000.

[4] A. Marvin, J. F. Dawson, S. Ward, L. Dawson, J. Clegg, and A. Weisenfeld, "A proposed new definition and measurement of the shielding effect of equipment enclosures", IEEE Transactions on Electromagnetic Compatibility, vol.46, no. 3, pp. 459-468, August 2004.

[5] IEEE Standard 299.1-2013. Method for Measuring the Shielding Effectiveness of Enclosures and Boxes Having all Dimensions between 0.1 m and 2 m,

[6] IEEE Standard 299-1997 for Measuring the Effectiveness of Electromagnetic Shielding Enclosures, 1997.

[7] H.A. Mendez, "Shielding theory of enclosures with apertures", IEEE Transactions on Electromagnetic Compatibility, vol. 20, pp. 296-305, May 1978.

[8] M.P. Robinson, J.D. Turner, D.W.P. Thomas, J.F. Dawson, M.D. Ganley, A.C. Marvin, S.J. Porter, T.M. Benson and C. Christopoulos, "Shielding effectiveness of a rectangular enclosure with a rectangular aperture", Electron. Lett., vol. 32, no. 17, pp. 1559-1560, August 1996.

[9] T. Konefal, J. F. Dawson, A. C. Marvin, M. P. Robinson, and S. J. Porter "A fast multiple mode intermediate level circuit model for the prediction of shielding effectiveness of a rectangular box containing a rectangular aperture", IEEE Transactions on Electromagnetic Compatibility, vol. 47, no. 4, pp. 678-691, November 2005.

[10] J.J. Shim, D.G. Kam, J.H. Kwon, H.D. Choi, J. Kim, "Circuital approach to evaluate shielding effectiveness of rectangular enclosures with apertures on multiple sides", International Symposium on Electromagnetic Compatibility, September 2004,Eindhoven.

[11] M. P. Robinson, T. M. Benson, C. Christopoulos, J. F. Dawson, M. D. Ganley, A. C. Marvin, S. J. Porter, and David W. P. Thomas, "Analytical formulation for the shielding effectiveness of enclosures with apertures", IEEE Trans. Electromag. Compat., vol. 40, no. 3, pp. 240-248, August 1998.

[12] R. Azaro, S. Caorsi, M. Donelliand, and G. L. Gragnani, "A circuital approach to evaluating the electromagnetic field on rectangular apertures backed by rectangular cavities", IEEE Trans. on Microwave Theory and Tech., vol. 50, pp. 2259-2266, August 2001.

[13] R. Azaro, S. Caorsi, M. Donelli, and G. L. Gragnani, "Evaluation of the effects of an external incident wave on metallic enclosures with rectangular apertures", Microwave Opt. Technol Lett 28 (2001), 289–293.

[14] S. V. Georgakopoulos, C. R. Birtcher, and C. A. Balanis, "HIRF Penetration Through Apertures: FDTD Versus Measurements", IEEE Trans. Electromag. Compat., vol. 43, no. 3, pp. 282-294, August 2001.

[15] F. Olyslager, E. Laermans, D. D. Zutter, S. Criel, R. D. Smedt, N. Lietaert, and A. D. Clercq, "Numerical and experimental study of the shielding effectiveness of a Metallic enclosure," IEEE Transactions on Electromagnetic Compatibility, vol. 41, pp. 202–212, August 1999.

[16] R. Azaro, S. Caorsi, M. Cosso, G. M. Costini, M. Donelli, R. Ene, G. L. Gragnani, and M. Pastorino, "A semianalytical approach for the evaluation of radiated immunity on a printed-circuit board in metallic enclosures", Microwave Opt Technol Lett 27 (2000), 204–207.

[17] R. De Smedt, J De Moerloose, S. Criel, D. de Zutter, F. Olyslager, E. Laermans, W. Wallyn and N. Lietaert, "Assessment of the shielding effectiveness of a real enclosure", International Symposium on Electromagnetic Compatibility, 14-18 September Rome, Italy. p.248-253, 1998.

[18] C. Christopoulos, the Transmission-Line Modelling Method- TLM, IEEE Press, New York, 1995.

[19] A. Taflove , S.C. Hagness , "Computational Electromagnetics: The FDTD Method", Artech House, 2000.

[20] Marcello D'Amore, and Maria Sabrina Sarto. "Theoretical and Experimental Characterization of the EMP-Interaction with Composite-Metallic Enclosures", IEEE Trans. Electromag. Compat., vol. 42, no. 1, pp. 152-163, February 2000.

[21] D. Fedeli, G. Gradoni, V. M. Primiani, F. Moglie, "Accurate Analysis of Reberveration Field Penetration Into an Equipment-Level Enclosure", IEEE Trans. Electromag. Compat., vol. 51, no. 2, pp. 170-180, May 2009.

[22] M. Clemens and T. Weiland, "Discrete Electromagnetism with the Finite Integration Technique", Progress In Electromagnetics Research, PIER 32, 65-87, 2001.

[23] J.M. Jing, "The Finite Element Method in Electromagnetics", John Wiley and Sons, 1993.

[24] R. Araneo and S. Celozzi , "Toward a Definition of Shielding Effectiveness in the Time Domain", IEEE International Symposium on Electromagnetic Compatibility, 5-9 Aug. 2013, Denver, CO, USA

[25] S. Celozzi and R. Araneo, "Alternative Definitions for the Time-Domain Shielding Effectiveness of Enclosures," IEEE Transactions on Electromagnetic Compatibility, Vol. 56, No. 2, Apr. 2014

[26] S. Celozzi and R. Araneo, "TD-Shielding Effectiveness of Enclosures in Presence of ESD", EMC Europe 2013, Brugge, Belgium, 2-6 Sep. 2013.

[27] Ludger Klinkenbusch, "On the Shielding Effectiveness of Enclosures", IEEE Trans. Electromag. Compat., Vol. 47, No. 3, pp. 589-601, August 2005

[28] R. Araneo, S. Celozzi, A. Tatematsu, and F. Rachidi, "Time-Domain Analysis of Building Shielding Against Lightning Electromagnetic Fields", IEEE Transactions on Electromagnetic Compatibility, Vol. 57, No. 3, Jun. 2015.

[29] J. Catrysse, and R. De Smedt, "Some Aspects of Shielding Effectiveness Related to Measurements and Simulations", IEEE International Symposium on Electromagnetic Compatibility, Vol. 1, pp. 480-485, Seattle, USA, Aug. 1999.

[30] Rohde and Schwarz, "R&S®ZVA / R&S®ZVB / R&S® ZVT Vector Network Analyzers Operating Manual", 1145.1084.12 ─ 18

[31] N. Dvurechenskaya, P. R. Bajurko, R. J. Zieliński, Y. Yashchyshyn, "Measurements of Shielding Effectiveness of Textile Materials Containing Metal by the Free-Space Transmission Technique with Data Processing in the Time Domain," Metrology and Measurement Systems, vol. 20, no. 2, pp. 217–228, Jun. 2013

[32] IEEE Standard P1597, Standard for Validation of Computational Electromagnetics Computer Modeling and Simulation – Part 1, 2 2008.

[33] A.P. Duffy, A.J.M. Martin, A Orlandi, G Antonini, T.M. Benson, M.S. Woolfson, "Feature Selective Validation (FSV) for validation of computational electromagnetics (CEM). Part I – The FSV method", IEEE Trans. on Electromagn. Compatibility, Vol 48, No 3, pp 449 – 459, Aug 2006.

[34] A Orlandi, A.P. Duffy, B Archambeault, G Antonini, D.E. Coleby, S Connor "Feature Selective Validation (FSV) for validation of

computational electromagnetics (CEM). Part II – Assessment of FSV performance", IEEE Trans. on Electromagn. Compatibility, Vol. 48, No 3, pp 460 – 467, Aug 2006,

[35] R. Araneo, G. Attolini, G. Lovat, and S. Celozzi, "A Global Approach to Time-Domain Shielding Problems", IEEE International Symposium on Electromagnetic Compatibility, pp. 86-90, Raleigh, USA, Aug. 2014.

Luis Ginés García-Pérez was born in Cartagena, Spain, in 1970. He received the Dipl. Ingeniero degrees in Industrial Engineering (Electronic and Automation specialty) from the Universidad de Murcia (UM), Murcia, Spain in 1995. He is freelance and his current research area is electromagnetic shielding. He is working towards his Ph. D.

Antonio José Lozano-Guerrero (M'13) was born in El Verger, Spain, in 1976. He received the Dipl. Ing. degree in Telecommunications engineering from the Universidad Politécnica de Valencia (UPV), Valencia, Spain in 2003 and his Ph.D. degree at the Universidad Politécnica de Cartagena (UPCT), Cartagena, Spain in 2008. From 2003 to 2004, he was a Research Assistant with the Department of Communications, UPV. In 2004, he joined the Department of Information Technologies and Communications, UPCT, where he is currently an Associate Lecturer. His current research areas are Electromagnetic Compatibility, Numerical Techniques in Electromagnetism and Industrial Microwave Heating Systems.

Juan Manuel Blázquez Ruiz was born in Cartagena, Spain, in 1990. He received the Dipl. Ing. degree in Telecommunications engineering from the Universidad Politécnica de Cartagena (UPCT), Cartagena, Spain in 2016. From 2014 to 2016, he worked on electromagnetic shielding effectiveness measurements in his final degree project.

Juan F. Valenzuela-Valdés was born in Marbella, Spain. He received the Degree in Telecommunications Engineering from the Universidad de Malaga, Spain, in 2003 and the Ph.D. from Universidad Politécnica de Cartagena, in May 2008. In 2004, he worked at CETECOM (Malaga). In 2004, he joined the Department of Information Technologies and Communications, Universidad Politécnica de Cartagena, Spain. In 2007, he joined EMITE Ing. as Head of Research. In 2011, he joined Universidad de Extremadura and in 2015, he joined Universidad de Granada where he is currently associate professor. His current research areas cover MIMO communications, smart antennas and wireless sensor networks. He has published over 70 papers in journals and conferences. Moreover, his Educational research interests include include collaborative learning, sustainability in education, and active learning methodologies.

Juan Monzó-Cabrera was born in Elda (Alicante), Spain, on January 1973. He received the Dipl. Ing. and Ph.D. degrees in Telecommunications engineering from the Universidad Politécnica de Valencia. He works nowadays as an Associate Lecturer at Universidad Politécnica de Cartagena. He has co-authored more than 60 papers in referred journals and conference proceedings and holds several patents regarding microwave heating processes. Dr. Monzó-Cabrera is the General Secretary of the Association of Microwave Power in Europe for Research and Education (AMPERE), a European association devoted to RF and microwave energy promotion. His current research areas cover microwave-assisted heating and numerical techniques in electromagnetism.

José Fayos-Fernández is currently an Associate Professor in the area of Signal Theory and Communications with the Universidad Politécnica de Cartagena (UPCT) since 2004. He received his PhD from UPCT in 2009. He received an MSc in Telecommunication Engineering from Universidad Politécnica de Valencia in 2001. He has enrolled with the Idaho State University (Pocatello, United States) in 2001, the IT'IS Foundation (Zurich, Switzerland) in 2006 and the Centro Tecnológico del Mármol, Piedra y Materiales (Cehegín, Spain) in 2013. His research is engaged towards metrology & experimental setup design, process optimization, electromagnetic (EM) material characterization, EM dosimetry and high power microwave applications.collaborative learning, sustainability in education, and active learning methodologies.

Alejandro Díaz-Morcillo (S'95-M'02-SM'09) received the Ingeniero (Ms. Eng.) and Doctor Ingeniero (Ph. D.) degrees in Telecommunication Engineering, both from Universidad Politécnica de Valencia (UPV), Spain, in 1995 and 2000, respectively. From 1996 to 1999 he was a Research Assistant at the Department of Communications of the UPV, and in 1999 he joined the Department of Information Technologies and Communications at the Universidad Politécnica de Cartagena (UPCT), Spain, as Teaching Assistant, where he is currently Professor since 2011. He leads the "Electromagnetics and Matter" Research Group at UPCT and his main research interest lays on Numerical Methods in Electromagnetics, Industrial Microwave Heating Systems and Dielectric Characterization.